Korean J. Chem. Eng., 37(7), 1199-1205 (2020)
DOI: 10.1007/s11814-020-0530-5

pISSN: 0256-1115
eISSN: 1975-7220

Evaluation of long-term stability in capacitive deionization using activated carbon electrodes coated with ion exchange polymers

Kyusik Jo*, Youngbin Baek,†, Seoni Kim*, Sung Pil Hong*, and Jeyong Yoon*,***,†**

*School of Chemical and Biological Engineering and Institute of Chemical Processes (ICP), Seoul National University, 1 Gwanak-ro, Gwanak-gu, Seoul 08826, Korea
**Department of Biotechnology, Sungshin Women's University, Seoul 01133, Korea
***Korea Environment Institute, 370 Sicheong-daero, Sejong-si 30147, Korea
(*Received 21 December 2019 • Revised 31 December 2019 • Accepted 28 February 2020*)

Abstract−Although capacitive deionization (CDI) is an energy-efficient and environment-friendly desalination technique, the severe performance decrease during long-term operation has been a critical obstacle to its practical application. Compared to various other approaches for stability improvement, the ion-exchange polymer (IEP) coating on the electrode seems to be both efficient and economically feasible. Nevertheless, there have only been limited studies aimed at understanding the role of IEP on stabilizing CDI operations. In this study, we investigated the effect of IEP on CDI performance by varying the amount of IEP coated on the electrodes. The polymer layer thickness was varied across the three IEP-coated electrodes used in this study (0, 30, and 100 μm). By monitoring the salt adsorption capacity (SAC) during the 50-h operation, it was found that the long-term stability of the system was dramatically improved upon using the IEP-coated electrodes. Additionally, the SAC retention was further improved with increasing IEP layer thickness. Based on the experimental analysis, we could conclude that the activated carbon particles' coating layer acted as a barrier to block the water molecules from the electrode surface, hence impeding carbon oxidation. The outer polymer layer formed on the electrode could additionally block the diffusion of oxygen sources from the bulk solution to the electrode, which further reduced the possibility of carbon oxidation. The results suggest that the IEP coating is effective towards maintaining the performance of the electrodes, and thicker IEP layers increased the electrode stability.

Keywords: Capacitive Deionization, Desalination, Long-term Stability, Ion Exchange Polymer Coating, Carbon Oxidation

INTRODUCTION

Capacitive deionization (CDI) is one of the latest desalination technologies [1]. The basic principle of CDI is to attract ionic species in the water into the porous electrode surface by applying low potential (i.e., <1.2 V) and forming an electrical double layer (EDL), and to release the adsorbed ions by applying reverse potential or zero potential. Unlike other desalination technologies such as reverse osmosis and distillation which need high pressure or heat and chemical substances for cleaning purposes, the CDI is both energy-efficient and eco-friendly. To achieve the industrial feasibility of CDI, many efforts have been made to improve its desalination performance [2-5].

However, various studies have reported degradation of CDI performance by more than 90% compared to its initial performance over several days of operation [6-8]. Considering that the long-term stability of the system is closely related to its cost and maintenance issues, the drastic performance degradation during long-term operation has hindered the practical application of CDI. The degradation in desalination capacity is due to the change in surface properties such as the potential of zero charge (PZC) shift induced from electrochemical carbon oxidation [9]. The carbon oxidation reaction is one of the side reactions that occur when the potential is applied in CDI [10,11]. In detail, carbon reacts with water molecules to form oxygen functional groups on the anode surface [12,13]. When the oxygen functional group is formed, the surface charge of the oxidation electrode is shifted in the positive direction, and the desalting capacity is reduced due to the imbalance of ion adsorption behavior between the anode and the cathode [14,15].

Many efforts have been made to improve CDI stability, including selection of different operation modes and application of functionalized materials. In the operation aspect, N_2 gas purging to the feed solution has been reported as an effective strategy for maintaining long-term operation performance because the carbon oxidation can be prohibited by reducing the dissolved oxygen concentration [6]. The other strategy was to use alternating potential in which applying positive potential (1.2 V for charging and 0 V for discharging) and negative potential (−1.2 V for charging and 0 V for discharging) resulted in reducing carbon oxidation on both electrodes [7]. Long-term stability was also improved by using membrane CDI (MCDI), which employs ion-exchange membranes in front of each electrode. In the material aspect, various researchers tried to introduce polymers or inorganic materials for stability improvement. Gao et al. [16,17] suggested the use of inverted CDI (i-CDI) by using electrodes with functional groups for tuning the surface charge to enhance the stability and salt adsorption capac-

†To whom correspondence should be addressed.
E-mail: jeyong@snu.ac.kr, ybbaek@sungshin.ac.kr

ity of the system. Srimuk et al. [18,19] introduced titanium oxide to the activated carbon electrode and found that the electrode stability was increased by suppressing H_2O_2 generation. Furthermore, Gao et al. [20] suggested the use of an ion-exchange-polymer-coated carbon anode, which showed stable desalination and higher charge efficiency compared to the pristine carbon electrode. According to this study, the ion-exchange polymer (IEP) coating on the carbon electrode can be a great option to enhance the CDI stability, considering its robust performance, high economic feasibility, and simple fabrication procedure. Nevertheless, scant studies have focused on studies for understanding the role of IEP in the CDI electrode.

In this study, we investigated the effect of the IEP on the CDI performance by varying the amount of IEP in the electrodes. By controlling of IEP coating level on the porous carbon electrode with different amount of IEP, three kinds of IEP-coated electrodes were prepared with different thicknesses of the polymer layer (0, 30, and 100 μm). The CDI performance was monitored over 150 cycles, and the performance of electrodes with different IEP layer thicknesses was compared. Electrochemical analysis was also conducted to investigate the electrical properties of electrodes before and after the operation, and the charge efficiency and energy consumption were also analyzed during the operations.

MATERIALS AND METHODS

1. Fabrication of Ion Exchange Polymer Coated Activated Carbon Electrode

The carbon electrode consisted of the activated carbon (MSP-20X, Kansai Coke and Chemicals, Japan), super P as a conductive material (Timcal co., Switzerland), and polytetrafluoroethylene as a binder (PTFE, Sigma-Aldrich, USA) at a weight ratio of 86 : 7 : 7, respectively. The three materials were mixed and kneaded together, and the mixture was pressed using a roll-pressing machine (MP200, Rotech, Republic of Korea). The electrode thickness was 300 μm. The specific surface area and the total pore volume of the activated carbon were 2,266 m^2/g and 0.79 cm^3/g, respectively, measured by the N_2 adsorption/desorption method (ASAP2010, Micromeritics, USA).

A cation-exchange polymer (CEP) and an anion-exchange polymer (AEP) were used as coating materials (INC-ICS for CEP and INC-ITA for AEP, Innochemtech, Republic of Korea). Note that the INC-ICS and INC-ITA are sulfonated and aminated polypropylene oxide (PPO), respectively, with 20% weight ratio. Each ion-exchange polymer solution in N-Methyl-2-pyrrolidone (NMP) was poured onto the fabricated electrode in a rectangular silicon mold (70 mm×40 mm×2 mm) located on the glass plate. Three kinds of IEP-coated electrodes were prepared by controlling the volumes of the IEP solution used. For example, 2 mL was chosen to percolate IEP solution into the AC electrode sufficiently so that AC particles inside the electrode were coated with IEP, but no extra layer was formed on the outer surface of the AC electrode. On the other hand, 3.5 and 5 mL were used to form the additional IEP layers with the thickness of 30 and 100 μm, respectively. After pouring, the electrodes with IEPs were kept at room temperature for 12 h followed by drying at temperatures below 70 °C for 12 h after removing the excess IEP solution. The IEP-coated electrodes were stored in deionized water and soaked in the feed solution, which was 10 mM NaCl solution before the desalination experiments.

2. Electrode Characterization

The morphology of IEP-coated electrodes with different coating layers was analyzed using a field-emission scanning electron microscope (FE-SEM, SUPRA 55VP, Carl Zeiss, Germany). Cyclic voltammetry (CV) analysis and electrochemical impedance spectroscopy (EIS) involved using a three-electrode cell. The cell consisted of a pristine activated carbon electrode or IEP-coated electrode as a working electrode either before or after long-term operation, referred to as 'OG' or 'LT', respectively, a carbon electrode four-times heavier than the working electrode as a counter electrode to avoid becoming a limiting electrode, and a reference electrode (Ag/AgCl (KCl sat'd.)). The CV was conducted in three cycles to measure the potential of zero charge (E_{PZC}) in the range from −0.4 V to 0.6 V (vs. Ag/AgCl (KCl sat'd.)), with a 2 mV s^{-1} scanning rate using a potentiostat (VersaSTAT 3, Princeton Applied Research, USA). The third cycle was chosen to find the potential of zero charge (E_{PZC}) from the average value of the potential at the minimum current passed during the oxidation step and the maximum current passed during the reduction step [8].

3. CDI Performance Test

CDI performance was evaluated using a typical CDI system, described elsewhere [21,22]. The CDI cell consisted of the circular type of either pristine electrodes or IEP-coated electrodes and a nylon spacer between a pair of electrodes. 10 mM NaCl solution was used as a feed solution and its flow rate was fixed at 2 mL min^{-1}. The electrical conductivity (3574-10C, HORIBA, Japan) and pH (9618-10D, HORIBA, Japan) of the effluent were measured in real time and the analyzed effluent was discarded. Note that the pH was measured to modify the effluent conductivity affected by H^+ and OH^-. Voltages of 1.2 V and 0 V were applied during the charging and the discharging steps, respectively, using a battery cycler (WBCS3000, WonATech, Republic of Korea) for 10 min. A charging/discharging cycle was repeated 150 times (a total of 50 h) to evaluate the long-term stability of CDI.

As representative desalination performance indicators, salt adsorption capacity (SAC) was calculated as follows [8,23]:

$$\text{SAC}\ (\text{mg g}^{-1}) = \frac{\text{Q}\cdot \text{M}_w \cdot \int(\text{C}_{in} - \text{C}_{out})\text{dt}}{\text{m}} \quad (1)$$

where C_{in} and C_{out} are the influent and effluent concentrations of NaCl (mM); Q is the flow rate (L min^{-1}); M_w is the molecular weight of NaCl (58.443 g mol^{-1}); dt is the time interval of the effluent concentration measurement; m is the electrode weight (g).

In addition, charge efficiency of CDI, the ratio of the charges consumed for adsorbing ions to total applied charges, was evaluated as follows [22]:

$$\text{Charge efficiency}\ (\%) = \frac{\text{Q}\cdot \text{F}\cdot \int(\text{C}_{in} - \text{C}_{out})\text{dt}}{\int \text{I}\text{dt}} \quad (2)$$

where I is the current at every second and F is Faraday constant. Note that Faraday constant was applied to convert the mass unit of the number of ions (mg) to the charge unit (coulomb, C).

RESULTS

1. Characteristics of Ion-exchange Polymer Coated Electrodes

Fig. 1 shows the cross-sectional SEM images for pristine electrodes and three kinds of IEP-coated electrodes prepared using different IEP solution volumes (2, 3.5, and 5 mL, respectively). When 2 mL of IEP was poured on the electrode, all the IEP percolated into the electrode. Therefore, as shown in Fig. 1(a) and (b), pristine and 2 mL IEP-coated electrodes showed similar macroscopic morphology. The small circular particles were super P, used as conductive additives for electrode fabrication. However, in the highly magnified SEM images (the inset figures from Fig. 1(a) and (b)), it was found that the smooth and clear surface of AC particles in the pristine electrode (Fig. 1(a)) changed to a coarse and porous surface, which shows that the AC particles were covered with IEP in the case of the 2 mL IEP-coated electrode (Fig. 1(b)). On the other hand, as the volume of introduced polymer increased, the IEP solution fully filled the interparticle space in the electrode, and the excess polymer made a polymer layer on the electrodes. Fig. 1(c) and 1(d) show the apparent IEP layer on the electrode, which has approximately 30 μm and 100 μm of thickness for the 3.5 mL and 5 mL IEP-coated electrode, respectively. Therefore, we named the

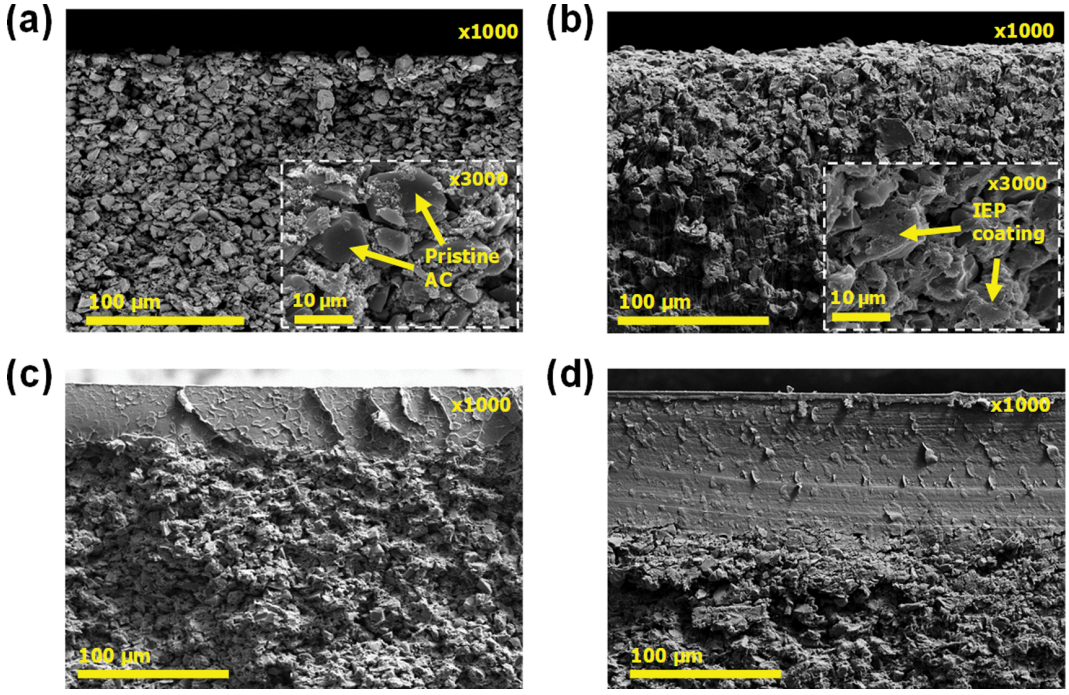

Fig. 1. Cross sectional SEM images of activated carbon electrodes: (a) Pristine electrode, ion-exchange polymer (IEP) coated electrode with (b) no outer layer (0 μm), (c) 30 μm and (d) 100 μm of outer layer. Inset figures in (a) and (b) are enlarged SEM image showing the surface of activated carbon particles.

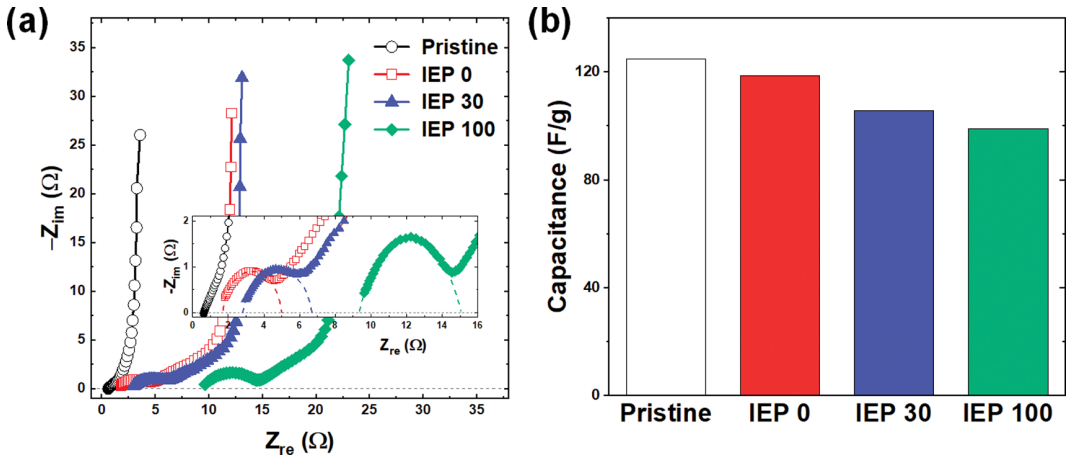

Fig. 2. (a) Nyquist plot and (b) capacitances of pristine and three ion-exchange polymer (IEP)-coated electrodes with thickness of 0, 30, and 100 μm (referred as IEP 0, IEP 30, and IEP 100, respectively). An inset figure in (a) is enlarged impedance profile at high frequency range. The capacitances were calculated from impedances in low frequency range (<20 mHz).

three kinds of IEP-coated electrodes after the thickness of the polymer layer: IEP-CCDI 0 for the electrode with 2 mL of IEP, IEP-CCDI 30 for the electrode with 3.5 mL of IEP, and IEP-CCDI 100 for the electrode with 5 mL of IEP.

Fig. 2 shows the Nyquist plot and capacitance of each electrode obtained by using EIS. Fig. 2(a) shows the half-circle profile in the Nyquist plot. The values of charge transfer resistance (R_{ct}), calculated from a radius of a half-circle in the Nyquist plot, for IEP-coated 0, 30, and 100 were 3.07 Ω, 3.24 Ω, and 4.75 Ω, respectively, and that for the pristine electrode was 1.54 Ω. In addition, equivalent series resistance (ESR), indicating the electrical resistance of the electrode, also increased as the thickness of IEP layer increased: 0.63, 1.55, 2.78, and 9.49 Ω for CDI, IEP 0, IEP 30, and IEP 100, respectively. Since these resistances are inversely related to both electrical and ionic conductivities of the electrodes, increased resistance with IEP indicates decreased conductivities, showing reduced capacitances with IEP (Fig. 2(b)) [24,25]. Fig. 2(b) shows the capacitances of four electrodes which were calculated from the impedances in the low frequency range (<20 mHz). As shown in the graph, the capacitance slightly decreased as the thickness of the IEP layer increased, which is ascribable to the decreased electrode conductivity. However, the difference of capacitance between the electrodes was quite small (<20%), which can lead to the expectation of minimal differences in initial desalination performance across all the prepared electrodes.

2. Long-term Stability in CDI using IEP Coated Electrodes

Using the pristine and three IEP-coated electrodes, we operated the CDI system at 150 cycles to evaluate the long-term stability of each electrode. Each cycle consists of 10 min of charging and 10 min of discharging, so the total operation time for each electrode was 50 h. SAC was calculated by conductivity change during the charging step in every cycle.

Fig. 3 shows the SAC values at the first cycle of operation with each electrode and the normalized SAC during the 150-cycle operations. As shown in Fig. 3(a), the SAC in the first cycle was increased when IEP was introduced into the electrode. The SAC also increased with increasing thickness of the IEP layer. The initial SAC in IEP-CCDI 0 was 16.8 mg g^{-1}, which increased to 18.0 mg g^{-1} in IEP-CCDI 30, and 19.0 mg g^{-1} in IEP-CCDI 100.

Fig. 3(b) shows how much SAC was retained during the 150-cycle operation. It was found that the desalination performance of the pristine electrode decreased drastically during the operation and the electrode became almost inoperable eventually at the 150-cycle. After the 150-cycle operation, the SAC in CDI had reduced by 99% and only 0.1 mg g^{-1} of adsorption capacity remained, indicating that the ions were barely adsorbed. However, compared to the pristine electrode, the long-term stability for IEP-coated electrodes was significantly improved regardless of the thickness of the IEP layer. The SAC of IEP-CCDIs decreased by only 12-20% over the 150 cycles, with 13.2-16.7 mg g^{-1} of SAC remaining after 50 h.

On the other hand, it was observable that the extent of SAC retention during operations was higher when the system was operated with the electrodes with thicker IEP layers. The SAC result operated in IEP-CCDI 100 showed the highest SAC retention (88%), which appeared to have the best long-term stability compared to IEP-CCDI 30 (81%) and 0 (80%).

3. Electrochemical Analyses

Fig. 4 shows the CV curves of both the IEP-coated electrodes and the pristine electrodes before and after the 150-cycle operation, used to compare carbon oxidation levels by measuring the potential of zero charge (PZC). As shown in Fig. 4(a), the PZC was shifted by 0.3 V after the operation, which is ascribable to carbon oxidation [9,20]. On the other hand, the PZC of IEP-coated electrodes showed smaller magnitudes of change compared to those of the pristine electrodes. As shown in Fig. 3(b), the PZC shifted by only 0.06 V for IEP-CCDI 0 and was even smaller for the electrodes with thicker IEP layers (0.03 V for IEP-CCDI 30 and 0 V for IEP-CCDI 100).

Fig. 5 shows the charge efficiency and the energy consumption during the operations. The charge efficiency was calculated by dividing the SAC by the electrical charge in both IEP-CCDI and CDI. As shown in Fig. 5(a), all IEP-CCDI showed charge efficiency greater than 80% while the charge efficiency in CDI significantly dropped from 60% to 0%. IEP-CCDI 100 showed the highest

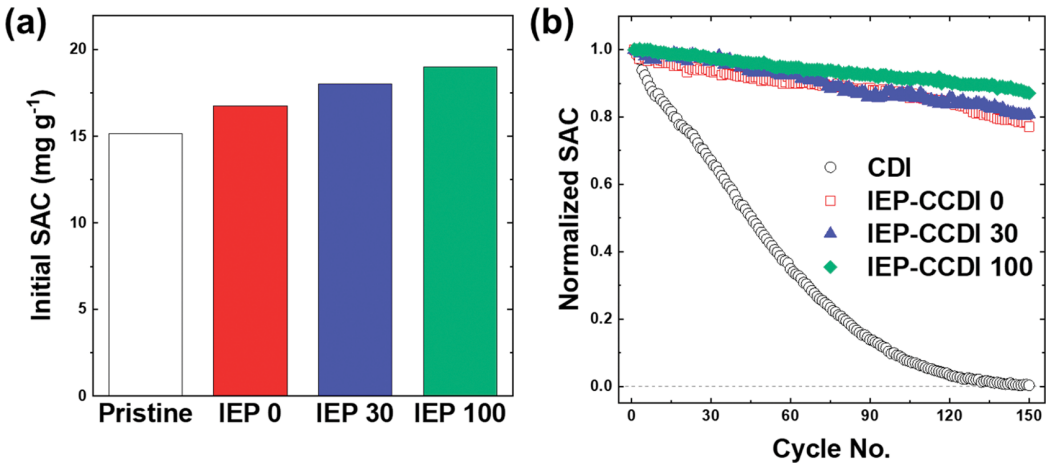

Fig. 3. (a) Salt adsorption capacity (SAC) of first cycle and (b) normalized SAC during 150 cycle operation of the CDI systems using pristine electrodes (referred to as CDI) and those using ion-exchange polymer (IEP)-coated electrodes with various outer thickness (referred to as IEP-CCDI 0, 30, and 100 for the electrodes having 0, 30, and 100 μm of outer IEP layer, respectively).

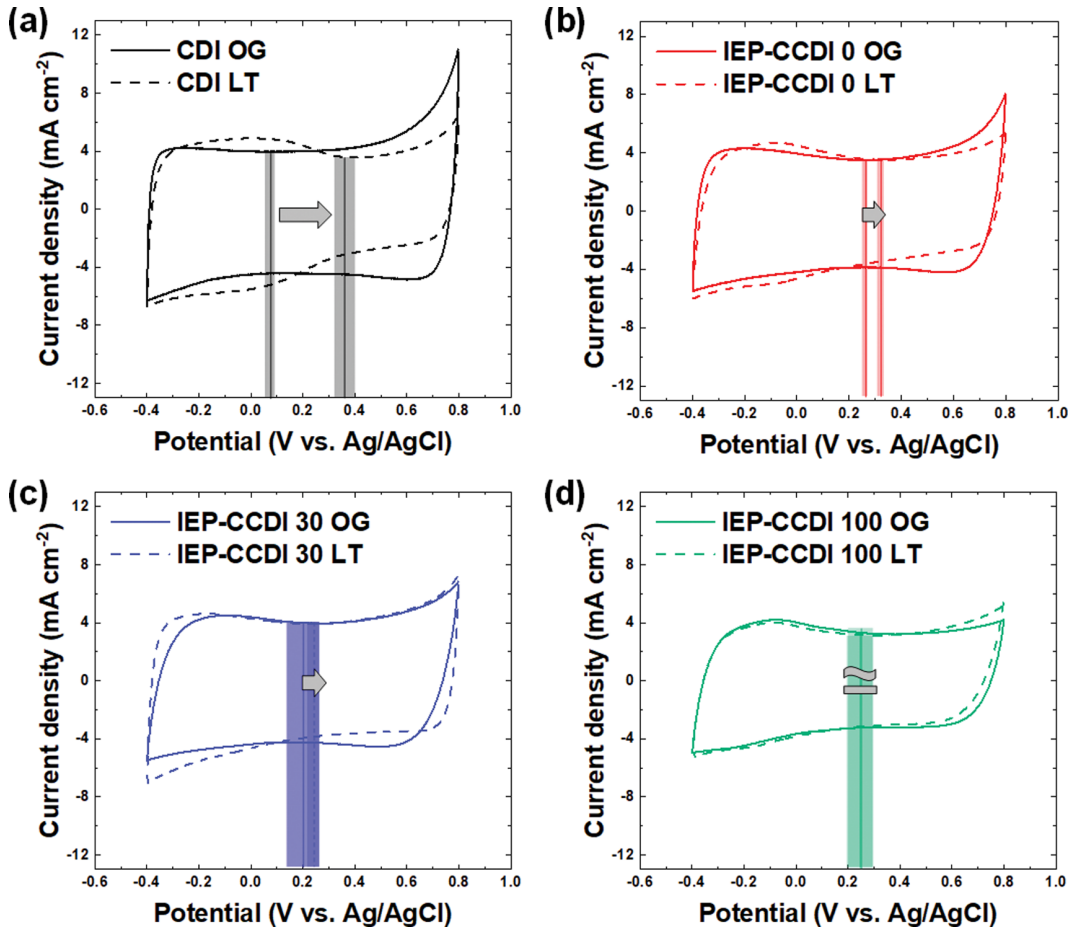

Fig. 4. Cyclic voltammetry of (a) CDI, (b) ion-exchange polymer (IEP)-coated CDI with 0 μm of IEP layer (IEP-CCDI 0), (c) IEP-CCDI 30, and (d) IEP-CCDI 100. The terms 'OG' and 'LT' indicate the electrodes before and after long-term operation, respectively. The vertical line means the potential of zero charge (PZC).

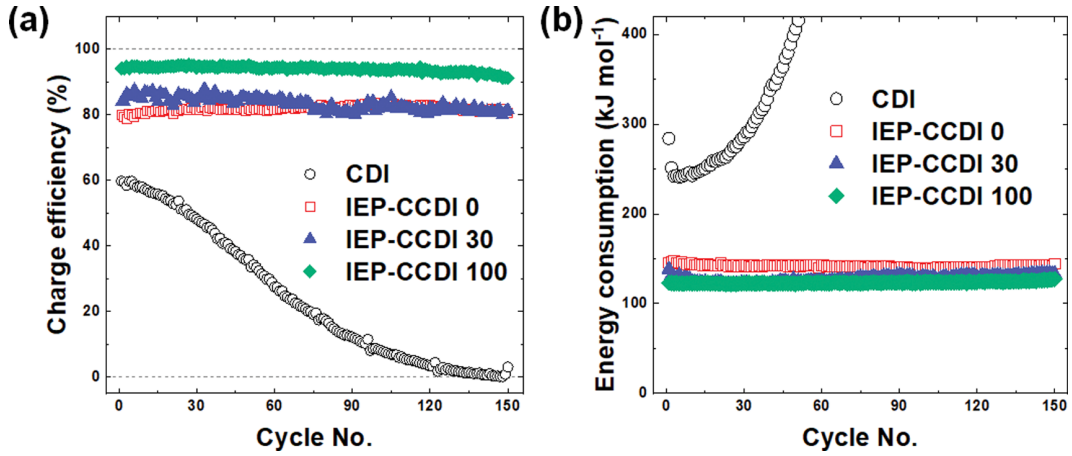

Fig. 5. (a) Charge efficiency and (b) energy consumption of CDI and three ion-exchange polymer (IEP)-coated CDI (IEP-CCDI) with variation in thickness (referred as IEP-CCDI 0, IEP-CCDI 30, and IEP-CCDI 100 for the CDI using the electrode having 0, 30, and 100 μm of thickness).

charge efficiency at 95% followed by approximately 80-85% for IEP-CCDI 0 and 30. Fig. 5(b) shows the energy consumption for 150 cycles of CDI and three IEP-CCDIs with variations in thickness. The energy consumption of CDI (approximately 240 kJ mol^{-1} initially) was higher than that of IEP-CCDI (123-145 kJ mol^{-1}) at the initial stage, and the gap increased during the 150-cycle opera-

tion. Among the three IEP-CCDI systems, energy consumption was very similar, but the energy consumption of IEP-CCDI 0 was the largest, followed by IEP-CCDI 30 and lastly IEP-CCDI 100. Additionally, the energy consumption shown to be 144, 133, and 127 kJ mol^{-1} for IEP-CCDI 0, IEP-CCDI 30, and IEP-CCDI 100, respectively, was rarely reduced after 150-cycle operation, while the CDI energy consumption increased sharply due to the large SAC reduction during long-term operation.

DISCUSSION

CDI is one of the promising desalination technologies in which an EDL is used for ion capture from water. For practical use, the evaluation of the system from a long-term perspective is mandatory. To increase the stability of the system, we coated the electrodes with IEP. As shown in the SEM images (Fig. 1), the voids between activated carbon particles were filled with IEP coating the particles, and the excess IEP formed an additional polymer layer on the electrode. Therefore, it could be observed that that the activated carbon particles were coated by IEP in all the IEP-coated electrodes regardless of the amount of IEP. On the other hand, polymer layers of different thicknesses (0, 30, and 100 μm) were formed on the electrode.

To evaluate the desalination performance of the electrodes, the SAC in the initial cycle of each electrode was compared. As shown in Fig. 3(a), the electrodes with thicker IEP layers showed higher SAC. This can be explained by the compensation of co-ion repulsion, which can also be found in membrane CDI [26-28]. When a charge barrier, the IEP layer was applied in this study, co-ions could not be repulsed out of the electrode followed by breaking of electroneutrality in the interparticle space (i.e., macropore) [26,29, 30]. Additionally, counter-ions are stored in the interparticle space to recover the electroneutrality of the space. Therefore, charges consumed to repulse co-ions could be compensated by the IEP layer [31,32], which improved the charge efficiency as shown in Fig. 5. These also appear that less Faradaic reactions occurred for the CDI with thicker IEP layer, which improves charge efficiency followed by the increase SAC by preventing charges from being dissipated. This effect could be dominant rather than increased overall resistance of electrodes, resulted in decreased capacitance with IEP layer (Fig. 2).

To evaluate the long-term stability of the electrode, the desalination performance of each electrode was monitored during 50 h of CDI operation (Fig. 3(b)). The results showed that the IEP coating on AC electrodes significantly enhanced the long-term stability, hence improving the performance of the IEP-coated electrodes compared to the pristine AC electrode; the performance was further increased when electrodes with thicker IEP layers were used. Even in IEP-CCDI 0, long-term stability was significantly increased compared to the pristine AC. Considering that the IEP-CCDI 0 did not have an outer IEP layer on the electrode surface, the increase in stability might be ascribable to the IEP percolated into the interparticle space, which was used for coating the AC particles. Thus, the coating layer on the AC particles reduced the rate of carbon oxidation. As discussed in the many literatures [8,12, 13,15,33], carbon can be oxidized by reacting with water molecules below 0 V potential [14]. Given that performance decrease mainly arises from the carbon oxidation, it is important to inhibit the approach of water molecules to the carbon surface to retain the performance over long-term operation. It seems that the IEP covering the AC particles can play an important role in inhibiting the approach of water molecules to the electrode surface. Therefore, IEP-coated electrodes have experienced less carbon oxidation, which could be verified from the PZC change at each electrode (Fig. 4). The PZC change of IEP-coated electrodes was approximately five-times lower than that of the pristine electrode, which indicates that the IEP-coated electrode experienced much lower oxidation compared to the pristine electrode.

Furthermore, as the thickness of the IEP layer on the electrode increases, higher rates of SAC retention are observed (Fig. 3(b)). The polymer layer formed on the electrode surface could block the diffusion of oxygen from the bulk solution to the electrode, which further reduces the possibility of carbon oxidation. The smaller PZC change for the operation using electrodes with thicker IEP layers (Fig. 4) confirms that the electrodes became more resistant to oxidation as more IEP was introduced. It is also possible that the extent of IEP coating on the activated carbons was differed from IEP 0, 30 and 100. Since different volumes of IEP solution were used to prepare those electrodes, less activated carbons inside of the electrode were coated with IEP in IEP 0 electrode while IEP 100 electrode was more filled with IEP. Therefore, these IEP coated electrodes increased overall resistance, which resulted in decreased capacitance but also increased desalination performance with fewer Faradaic reactions.

By using IEP-coated electrodes, the system showed a higher charge efficiency and lower energy consumption. Given that the lower charge efficiency implies that larger charge was consumed by the unwanted side reactions (e.g., carbon oxidation), the higher charge efficiency observed in IEP-coated electrodes is in good agreement with the trend of the SAC retention rate (Fig. 3) and the PZC change of electrodes (Fig. 4). This IEP coating could be effective to reduce the energy consumption of the system by improving charge efficiency.

As discussed, IEP-CCDI 100 showed the best desalination performance (i.e., initial SAC and long-term stability); therefore, it is expected that the thicker the IEP layer, the higher is the performance. However, one must still consider the cost of IEP from the perspective of a real application. For example, the cost of IEP is approximately \$8.4 m^{-2} which is over 90% of the entire electrode material cost (\$10 m^{-2}), considering that the prices of IEP and AC were approximately \$120 L^{-1} and \$10 kg^{-1}, respectively, when fabricating IEP-coated electrodes with 30 μm of the IEP layer. Furthermore, the fabrication cost of the IEP-coated electrode 100 increases to up to three-times that of the IEP-coated electrode 30. In addition, the cost of the CDI module casing should also be increased. Therefore, the thickness of the IEP layer should be optimized by considering both the desalination performance and the cost.

CONCLUSION

We investigated the effect of the IEP on the CDI performance.

By varying the amount of IEP used for coating, three IEP-coated electrodes were prepared with different thicknesses of polymer layers (0, 30, and 100 μm). In the IEP-coated electrodes, activated carbon particles inside the electrodes were coated with IEP. By observing the desalination performance of each electrode for 50 h, we found a significant increase in the system stability for the IEP-coated electrodes compared to pristine electrodes. In addition, the stability was further improved with the application of thicker IEP layer electrodes. From further analysis, we found that the coating layer of activated carbon particles impeded carbon oxidation by inhibiting the approach of the water molecules to the electrode surface. The outer polymer layer on the electrode prohibited the diffusion of oxygen sources from the bulk solution to the electrode, which further reduced the possibility of carbon oxidation. By analyzing the charge efficiency and energy consumption of the system, we could conclude that the IEP coating on the electrode can improve the energy efficiency of the CDI system.

ACKNOWLEDGEMENTS

This work was supported by the Technology Innovation Program (10082572, Development of Low Energy Desalination Water Treatment Engineering Package System for Industrial Recycle Water Production) funded by the Ministry of Trade, Industry, and Energy (MOTIE, Korea) and by the National Research Foundation of Korea (NRF) grant funded by the Ministry of Science, ICT and Future Planning (NRF-2018R1C1B5086300).

REFERENCES

1. M. E. Suss, S. Porada, X. Sun, P. M. Biesheuvel, J. Yoon and V. Presser, *Energy Environ. Sci.*, **8**, 2296 (2015).
2. J.-Y. Choi and J.-H. Choi, *J. Ind. Eng. Chem.*, **16**, 401 (2010).
3. C. Tsouris, R. Mayes, J. Kiggans, K. Sharma, S. Yiacoumi, D. DePaoli and S. Dai, *Environ. Sci. Technol.*, **45**, 10243 (2011).
4. B. Jia and L. Zou, *Chem. Phys. Lett.*, **548**, 23 (2012).
5. M. T. Z. Myint and J. Dutta, *Desalination*, **305**, 24 (2012).
6. Y. Bouhadana, E. Avraham, M. Noked, M. Ben-Tzion, A. Soffer and D. Aurbach, *J. Phys. Chem. C*, **115**, 16567 (2011).
7. I. Cohen, E. Avraham, Y. Bouhadana, A. Soffer and D. Aurbach, *Electrochim. Acta*, **106**, 91 (2013).
8. J. Yu, K. Jo, T. Kim, J. Lee and J. Yoon, *Desalination*, **439**, 188 (2018).
9. E. Avraham, M. Noked, Y. Bouhadana, A. Soffer and D. Aurbach, *Electrochim. Acta*, **56**, 441 (2010).
10. T. Kim, J. Yu, C. Kim and J. Yoon, *J. Electroanal. Chem.*, **776**, 101 (2016).
11. J.-H. Lee, W.-S. Bae and J.-H. Choi, *Desalination*, **258**, 159 (2010).
12. A. Omosebi, X. Gao, J. Landon and K. Liu, *ACS Appl. Mater. Interfaces*, **6**, 12640 (2014).
13. Y. Bouhadana, M. Ben-Tzion, A. Soffer and D. Aurbach, *Desalination*, **268**, 253 (2011).
14. C. Zhang, D. He, J. Ma, W. Tang and T. D. Waite, *Water Res.*, **128**, 314 (2018).
15. D. He, C. E. Wong, W. Tang, P. Kovalsky and T. D. Waite, *Environ. Sci. Technol.*, **3**, 222 (2016).
16. X. Gao, A. Omosebi, J. Landon and K. Liu, *Energy Environ. Sci.*, **8**, 897 (2015).
17. X. Gao, A. Omosebi, J. Landon and K. Liu, *Environ. Sci. Technol.*, **49**, 10920 (2015).
18. P. Srimuk, L. Ries, M. Zeiger, S. Fleischmann, N. Jäckel, A. Tolosa, B. Krüner, M. Aslan and V. Presser, *RSC Adv.*, **6**, 106081 (2016).
19. P. Srimuk, M. Zeiger, N. Jäckel, A. Tolosa, B. Krüner, S. Fleischmann, I. Grobelsek, M. Aslan, B. Shvartsev, M. E. Suss and V. Presser, *Electrochim. Acta*, **224**, 314 (2017).
20. X. Gao, A. Omosebi, N. Holubowitch, A. Liu, K. Ruh, J. Landon and K. Liu, *Desalination*, **399**, 16 (2016).
21. K. Jo, Y. Baek, C. Lee and J. Yoon, *Appl. Sci.*, **9**, 5055 (2019).
22. J. Kang, T. Kim, K. Jo and J. Yoon, *Desalination*, **352**, 52 (2014).
23. J. Kang, T. Kim, H. Shin, J. Lee, J.-I. Ha and J. Yoon, *Desalination*, **398**, 144 (2016).
24. A. J. Bard and L. R. Faulkner, *Electrochemical methods: fundamentals and applications*, Wiley, New York (2000).
25. J.-H. Jang and S.-M. Oh, *J. Korean Electrochem. Soc.*, **13**, 223 (2010).
26. P. M. Biesheuvel and A. van der Wal, *J. Membr. Sci.*, **346**, 256 (2010).
27. S. Porada, L. Weinstein, R. Dash, A. van der Wal, M. Bryjak, Y. Gogotsi and P. M. Biesheuvel, *ACS Appl. Mater. Interfaces*, **4**, 1194 (2012).
28. P. Długołęcki, B. Anet, S. J. Metz, K. Nijmeijer and M. Wessling, *J. Membr. Sci.*, **346**, 163 (2010).
29. R. Zhao, O. Satpradit, H. H. Rijnaarts, P. M. Biesheuvel and A. van der Wal, *Water Res.*, **47**, 1941 (2013).
30. M. D. Andelman and G. S. Walker, US Patent, 6,709,560 (2004).
31. A. Jain, J. Kim, O. M. Owoseni, C. Weathers, D. Cana, K. Zuo, W. S. Walker, Q. Li and R. Verduzco, *Environ. Sci. Technol.*, **52**, 5859 (2018).
32. Y.-J. Kim and J.-H. Choi, *Sep. Purif. Technol.*, **71**, 70 (2010).
33. S. Maass, F. Finsterwalder, G. Frank, R. Hartmann and C. Merten, *J. Power Sources*, **176**, 444 (2008).